

Partitioned Reconstruction of Contact Forces in Tactile Sensor Arrays for Robotic Sensing Systems

María-Luisa Pinto-Salamanca^a and Wilson-Javier Pérez-Holguín^b

Doctoral Program in Engineering with an emphasis in Electronics Engineering, School of Electronic Engineering, GIRA Research Group, Universidad Pedagógica y Tecnológica de Colombia UPTC, Colombia

Keywords: Tactile Sensing, Contact Forces Reconstruction, Tactile Sensor Array, Force Sensors, Robot Sensing Systems.

Abstract: The reconstruction of contact forces is essential for the performance of robotic manipulation systems from the information captured by tactile sensors. This work explores the implementation of a model-driven approach for the triaxial reconstruction of contact forces in tactile sensor arrays using a partition algorithm that estimates forces in smaller subarrays on a flat and rigid surface. The validation of the presented approach depends on a prior verification of compliance with the centroids of traction and compression for each analysed subarray. Considering the force estimation errors, the proposed approach shows a better behaviour than similar works for single contacts in the force reconstruction for multiple contact events and when using large size sensors arrays. In addition, the application of the partitioning approach demonstrates a significant decrease in response time by reducing the number of operations that are needed for the force reconstruction calculation. Although the relative errors are still significant, the results obtained allow verifying a clear contribution to the reconstruction of contact events under processing time restrictions for sensor arrays ranging from small to large scale, that favors the development of electronic skin in robotic applications.

1 INTRODUCTION

The feedback of forces and the perception of contact events in real-time play a fundamental role in the planning of the robot's interactions with the environment (Lambeta et al., 2020) as well as in the grip or slip control loops (Masoumian et al., 2020). Likewise, forces estimation is essential for robotic manipulation and human-robot interaction since the obtained force components allow a complete description of a contact phenomenon (Ciotti et al., 2019).

To replicate the human sense of touch, tactile sensing systems employ a tactile sensor layer, an electronic interface layer, and a tactile data decoding system (Dahiya, et al., 2010), (Ibrahim et al., 2017). Tactile sensing systems allow performing tasks as tactile exploration, object identification, and object grasping and movement. Tactile perception contributes to expanding the capabilities of robotic manipulators, humanoid robots, and biomedical devices, among other applications. An example of

that is the combination of robotics with tactile sensing systems, which provides emulation functions of fingers perception in sophisticated manipulation of dexterous grippers in hand robots or manipulators (Y. Li et al., 2019).

Considering the contact medium, tactile sensors can be continuous or discrete. In particular, discrete tactile sensors are usually organized as arrays of individual sensors that can simultaneously be activated in response to a contact event (Mohammadi et al., 2019).

The basic unit in tactile sensor arrays is known as 'taxel', which is in charge of measuring a contact event in a single point (Dahiya et al., 2010). Tactile sensors can also be configured as arrays of taxels to cover flat areas (Seminara et al., 2015), hard or soft surfaces (Yuan, et al. 2017), or deformable areas (Ciotti et al., 2019). Some sensor arrays offer three or six-axis force estimation with sensing areas up to 4.7mm × 4.7mm with 24 taxels (XELA Robotics Inc). However, most sensor arrays measure stress or normal force. In such cases, additional processing steps are required to decode triaxial forces.

^a  <https://orcid.org/0000-0002-2089-0683>

^b  <https://orcid.org/0000-0001-5238-4470>

The contact forces reconstruction process allow obtaining the force distribution on a surface from tactile sensor measures (Seminara et al., 2015) using analytical models based on physical laws (model-driven), machine learning frameworks (data-driven) (Wasko et al., 2019), and mixed approaches. Sensors employed with such approaches comprehend vision-based, piezoresistive, magnetic, piezoelectric, Hall Effect, and biomimetic technologies.

Some applications of forces estimation in the robotics field include shape-recognition in robot-objects interaction (X. Li et al., 2020), wearable assist robots (Ito et al., 2019), grasping object in robotic hands (Mohammadi et al., 2019), human-robot interaction (Cirillo et al., 2016), robotic skin (Trueeb et al., 2020), and soft artificial skin (Duong & Ho, 2021), among others.

In tactile sensing systems, there are different contact sensing areas for electronic skin applications covering from small to large scales, depending on the resolution and number of taxels in the sensor array. Seminara et al. (2015) cover an area close to $36\text{mm} \times 36\text{mm}$ using a 3mm thick elastomer layer and a sensor grid of 10×10 piezoelectric taxels. Duong & Ho (2021) pose a vision-based model using a FEM analysis to establish the relationship between nodal displacements of the markers and external forces achieving to cover an area of 49763mm^2 . However, in the case of works focused on vision, the sensors' size, and the dependence on complex image processing algorithms, make it difficult to extend its use to large artificial skin development in portable robotics or biomedical applications.

Proper emulation of the human sense of touch involves meeting a strict time limit to detect contact events and process them in less than 1 ms (Dahiya, et al., 2010). A challenge for applications using a discrete array of sensors is to achieve a reasonable compromise between the execution speed and the accuracy of the results, considering the need for developing calibrating algorithms and parallel process scenes of complex contact events in real-time.

There are few works in the literature (Seminara et al., 2015), (Cimino, 2016) centered on the real-time implementation of force reconstruction algorithms employing sensor arrays. These authors propose the reconstruction of triaxial contact force distributions on a soft layer surface from the normal stress data retrieved from a piezoelectric sensor array. Although this work could be used with other sensor arrays whose taxels provide discrete stress data, its application has not been generalized.

This work analyzes, at the simulation level, the implementation of the model-driven proposed by Seminara et al. (2015) to reconstruct contact forces in tactile sensor arrays with a partitioned approach, considering smaller subarrays. The partitioning approach was applied to arrays of sensors of different resolutions ranging from 10×10 to 48×48 taxels to covering different contact areas. This approach is aimed to reduce the computational load that allows speeding up the calculation times required for the reconstruction of forces. Although the errors obtained are relatively high, it is expected that combining this approach with a hardware implementation (FPGA-like) will achieve compliance with the 1 ms limit in tactile sensor applications using large arrays of normal stress sensors.

2 MATERIALS AND METHODS

2.1 Contact Forces Estimation for Tactile Sensor Arrays

The model-driven approach proposed by Seminara et al. (2015) allows the estimation of the intensities and directions of contact forces (three-dimensional force) starting from normal stress data of a discrete tactile sensor (single-dimensional data). This is relevant because this approach would extend the application of normal stress tactile sensors to the triaxial forces estimation. The Seminara et al. (2015) model is based on the solution to the inverse problem of the Boussinesq equation for an elastic half-space (Johnson, 1985). This model estimates force vectors in the same taxels XY -coordinates, on the sensor cover layer at a distance h on the z -axis (sensor thickness).

This model establishes that the triaxial forces components (x_1 force in x -axis, x_2 force in y -axis, and x_3 force in z -axis) are defined as:

$$\begin{bmatrix} x_1 \\ x_2 \\ x_3 \end{bmatrix} = C^\dagger b + (I - C^\dagger C) w \quad (1)$$

where, b is a normal stress vector sensed by the taxels in the sensor array, C is a matrix defined by the vector distances given between the taxels coordinates and the points where the force vectors are reconstructed, C^\dagger is the Moore-Penrose pseudo-inverse matrix of C (Albert, 1972), and w is a vector that depends both on two continuous scalar variables μ_1 and μ_2 , as well as on the geometry and the sensor input data.

The values for μ_1 and μ_2 are defined to maximize an Π objective function that simultaneously fulfils three physical restrictions: *i*) compressive normal forces, *ii*) tangential forces and normal forces similarly distributed over the contact area, and *iii*) no pinch.

The Seminara et al. (2015) model proposes two stages to define the objective function (called preparative phase) and find the optimal solution (called iterative phase). The preparative phase includes calculating the matrices, reading the data from the tactile sensor, and calculating the centroids required to establish the physical constraints and the objective function. The iterative phase allows finding the values of μ_1 and μ_2 that optimize the Π function. By a comparison between a FEM simulation and the analyzed model, the maximum estimated errors were about 13% in the resultant tangential forces for Hertzian contacts and 43% of the resultant force in the x -axis for non-Hertzian contacts (Seminara et al., 2015).

The mentioned model was evaluated through a software implementation conducted in Matlab® R.2020b, by varying the sensor parameters, the taxels data and the force coordinates. Figure 1 shows a case of force reconstruction for a tactile sensor array of 10×10 taxels with $4\text{mm} \times 2\text{mm}$ resolution in the XY -plane and 3mm thickness. For this example, the normal stress data values read by the sensor are between $-36000 \text{ [N/m}^2\text{]}$ to $20912 \text{ [N/m}^2\text{]}$. These were obtained experimentally by applying the function:

$$S(x, y) = 1 \times 10^6 * (y \sin(100x) + x \cos(100y)) \quad (2)$$

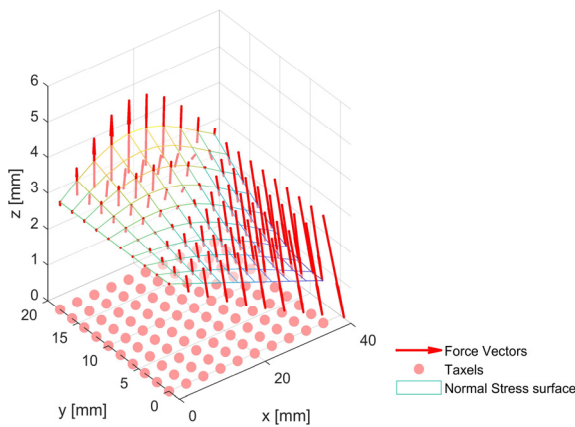


Figure 1: Contact forces reconstruction applying the model-driven proposed by (Seminara et al., 2015). Scale factors: $F_x=10000 \text{ [N/mm]}$, $F_y=10000 \text{ N/mm}$, $F_z=1 \text{ [N/mm]}$, Normal stress surface = $0.003 + S * 20000 \text{ [N/m}^2\text{]}$.

2.2 Partitioning Approach to the Forces Estimation

The partitioning approach proposed involves sectioning the tactile sensor array into subarrays of equal size and applying the force reconstruction algorithm proposed by Seminara et al. (2015) in each subarray as if they were independent sensors. Then, these are grouped together to obtain the overall response of the force estimates.

Although it is clear that the principle of superposition cannot be applied to a non-linear model, the sharp decrease in the size of the operations of the matrix and its consequent decrease in the system's response time justify the evaluation of the proposed approach. This approach should be used considering the accuracy requirements for force estimation, which may vary in each case.

The algorithm to implement the model-driven of Seminara et al. (2015) has a computational complexity of $O(d^2)$ order, where d is the size of the tactile sensor array (Wasko et al., 2019). The model application implicates matrix operations of $3(n_{ht} \times n_{vt}) \times 3(n_{ht} \times n_{vt})$ order, where n_{ht} and n_{vt} are the number of horizontal and vertical taxels in the array. Hence, if the size of the array decreases, the calculation time also decreases. Figure 2 shows four partition cases to be considered in the proposed approach that include:

- Case 0: the reconstruction of forces in a sensor array without a subarray (SA0 1×1)
- Case 1: mix of the cases above with four subarrays SA1-SA4 (2×2 subarrays).
- Case 2: two vertical subarrays SA1-SA2 (1×2)
- Case 3: two horizontal subarrays SA1-SA2 (2×1)

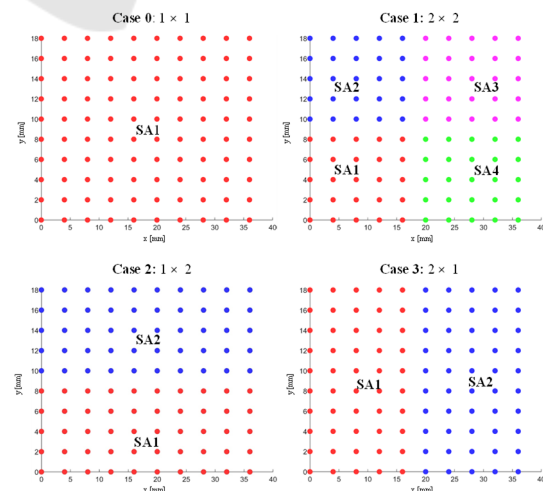


Figure 2: Partition Cases Analyzed in the Contact Force Reconstruction Approach.

The performed tests comprise four tactile sensor arrays whose characteristics are described in Table 1. For the cases of 10×10 taxel matrices, normal stress data corresponding to Hertzian and non-Hertzian contact events were the same used by (Seminara et al., 2015). In the 20×20 taxel array, the sensor input data were combinations of Hertzian and non-Hertzian contacts. The input data for the 48×48 array were obtained with an FSR Matrix Array Sensor for the plantar pressure measurement systems (PPMs) described in (Castro et al., 2020).

Table 1: Included Sensors for the implementation of the partitioned approach.

Tactile Sensor	Taxels Array ($n_{ht} \times n_{vt}$)	Size [mm \times mm \times mm]	Taxels Separation Resolution [mm \times mm]
Sensor 1	10×10	$20 \times 40 \times 3$	4×2
Sensor 2	10×10	$40 \times 40 \times 3$	4×4
Sensor 3	20×20	$20 \times 40 \times 3$	4×2
Sensor 4	48×48	$384 \times 384 \times 0.91$	8×8

The search for the optimal parameters μ_1 and μ_2 was carried out using the Matlab® function *fmincom*. The objective function Π is conditioned for the centroids of the contact event (*Centroids Condition*) such that: the data detected in the matrix must include positive and negative values to calculate the compression and tension centroids simultaneously. Consequently, the partitioning approach initially checks for this condition on the data in the subarray. If this condition is met, the approach try to perform as much partitionings as possible.

In the proposed approach the preparatory phase of each partitioning case comprises: *i*) separate stress data from each partition, *ii*) redefine the coordinates of the taxels and the force estimation, *iii*) calculate the C matrix and the C^\dagger pseudo-inverse matrix for each subarray, *iv*) determine the centroids of tension and compression for each subarray, and finally *v*) evaluate the Π functions.

The iterative phase for each analyzed partition includes two stages: *i*) find the optimal values to the parameters μ_1 and μ_2 for each analyzed subarray, and *ii*) compare the minimum forces obtained with an established threshold. Finally, the algorithm groups the reconstructed forces to present a force vector for each taxel.

3 ANALYSIS OF RESULTS

The simulations carried out applying the proposed approach generate the estimation errors presented in

Table 2, according to cases 0 to 3 described in the previous section and the sensor parameters shown in Table 1. The resulting forces correspond to the sum of the estimated forces in each axis ($X_1 = \sum x_1$, $X_2 = \sum x_2$, $X_3 = \sum x_3$). The error was calculated as:

$$Error = \frac{Ref. value - Resultant Force}{Ref. value} \quad (3)$$

For the force reconstruction using sensors 1 and 2, the reference values for error estimation were obtained by mean a FEM simulation developed in COMSOL® by Seminara et al. (2015). In the analysis carried out with sensors 3 and 4, the estimation error was similar to those obtained for Case 0 (without partitioning). Due to the application of Equation 3, Table 2 contains some negative values for the error.

Table 2: Estimation errors obtained during the partitioning approach validation.

Sensor	Analysis Case	Estimation errors		
		X_1	X_2	X_3
1	0	12.84%	12.93%	7.54%
	1	77.52%	65.69%	-23.57%
	2	46.32%	71.17%	-15.15%
	3	64.41%	5.60%	-0.46%
2	0	-39%	16%	-1%
	1	17.52%	51.22%	-11.60%
	2	-97%	55%	-5%
	3	42%	-1%	-7%
3	0	0%	0%	0%
	1	3.91%	-12.67%	-1.37%
	2	0.11%	0.07%	-1.15%
	3	5.05%	-12.05%	-0.23%
4	0	0%	0%	0%
	1	51.04%	68.98%	-5.44%
	2	49.10%	-63.09%	-5.21%
	3	51.61%	-67.72%	-4.25%

Figure 3 shows a comparison between the optimal values μ_1 and μ_2 for each case. During the approach validation, the μ values for the partition Case 0 is taken as reference. For the partitions that do not meet the centroid conditions, the values of μ_1 and μ_2 are null. The response of the partitioning approach is analyzed by classifying the contact events as ‘simple’ for sensors 1 and 2 and ‘multiple’ for sensors 3 and 4.

3.1 Single Contacts

Figure 4 shows the reconstruction cases when using sensors 1 and 2. In the case of the sensor 1 (Figure 4(a)), the input data corresponds to a single Hertzian-

type contact event. As shown in Figure 3, for Case 1, two subarrays (SA2 and SA4) do not meet the centroid conditions, so their optimal parameters were null. Figure 3 also shows that Case 2 do not fully comply with the contact conditions. During the test with sensor 1 and Case 3 forces are estimated in the two subarrays taking into account that μ_1 and μ_2 are different to zero. However, it would be noted that this case present a high estimated error (64.41%) in the

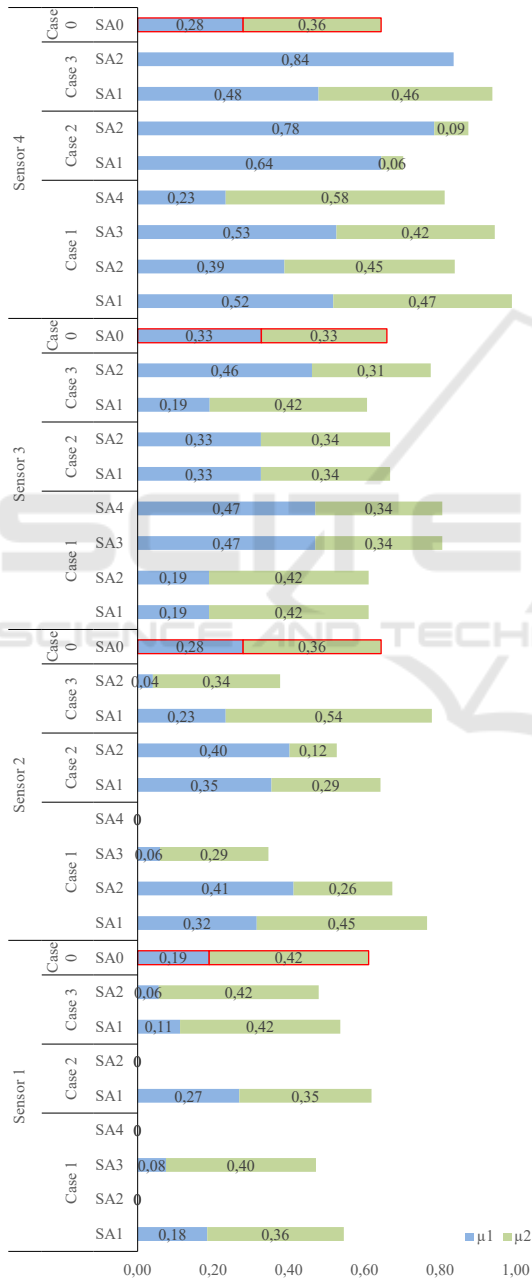


Figure 3: Flow diagram for implementation of the partitioning approach for the contact forces reconstruction.

resulting forces on the x -axis, while the reference (Case 0) gives a maximum estimation error of about 13% for the tangential forces. The results obtained allow verifying that the proposed partition strategy does not work correctly in the case of single contact and Hertzian events.

For sensor 2, the input data corresponds to a non-Hertzian contact (Figure 4(b)). For Case 1, it is observed that the centroid condition is not fulfilled in subarray SA4. For partitions with two subarrays, the estimation errors for Case 3 show a better performance than Case 2. If Case 3 is compared with the reference (Case 0), the first one present a smaller error in the resultant force on the y -axis (1%). However, for these cases the forces estimation error with respect to the z -axis is better for Case 0 (-1% vs. -7%). Since the non-Hertzian contact is a simple contact located in the center of the sensor, the centroid condition is fulfilled more easily than in the Hertzian case.

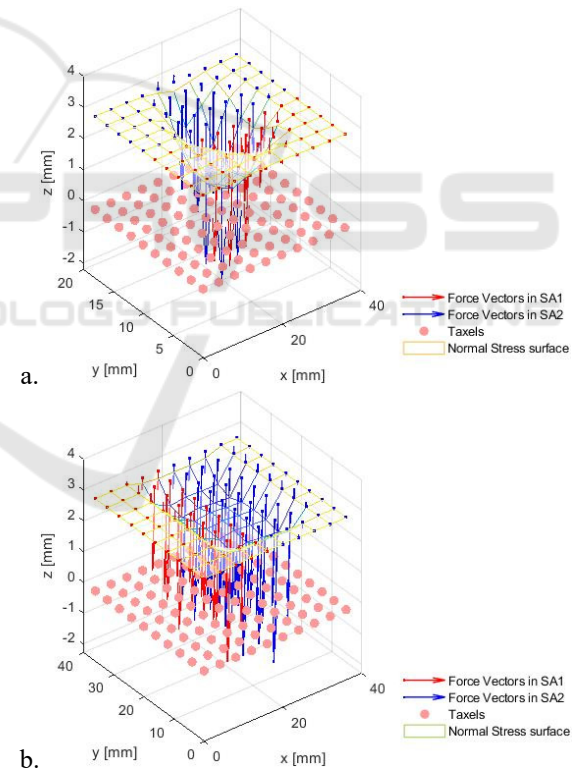


Figure 4: Results of partitioned force reconstruction. a) Hertzian contact Case 2, b) Non-Hertzian contact Case 3.

3.2 Multiple Contacts

Figure 5 and 6 present the results of applying some cases of force reconstruction for sensors 3 and 4, respectively. The input data used with sensor 3 (see

Figure 5) are combinations of two Hertzian and non-Hertzian contacts. Based on the estimation errors, the input data for sensor 3 exhibits the best performance for the partitioning approach. Although Case 1 fulfilled the centroid conditions for all partitions, the errors given for Case 2 are lower, so Case 2 is the best choice to be employed in the proposed approach with the multiple Hertzian and non-Hertzian contact event.

Regarding the reconstruction of forces with sensor 4 (see Figure 6), all the partition cases fulfilled the centroid conditions. However, Case 3 present the lowest estimation errors for the resulting force in the z -axis (-4.25%), so this case is the best for the analyzed contact event with sensor 4. For this sensor, in each case of analysis, the response times of the algorithm were evaluated, obtaining the data presented in Figure 7. Executing the algorithm with one partition (Case 0) requires 2705.33s, with two subarrays, Cases 2 and 3, it takes 354.17s and 330.57s, respectively, while with four subarrays (Case1) it only requires 109.63s. Figure 7 also shows three tests for the same partitioning case which generated similar response times for each test.

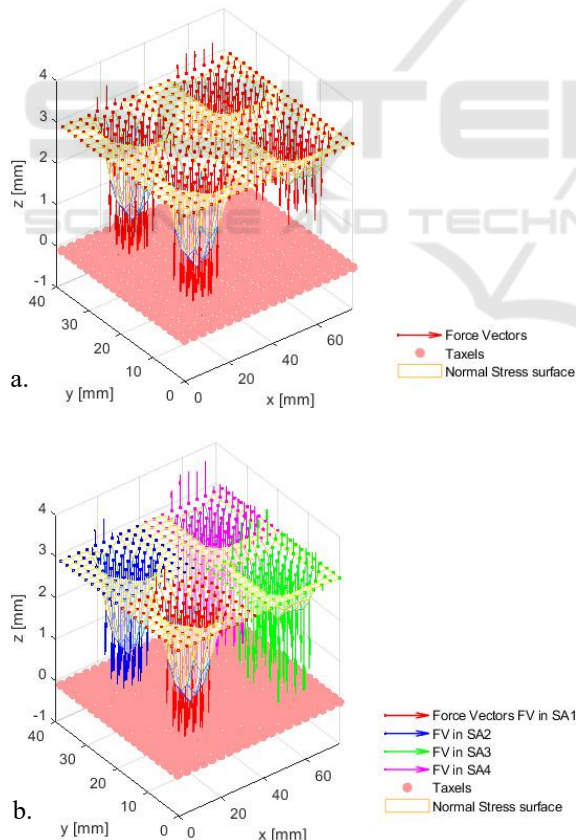


Figure 5: Results of partitioned force reconstruction in multiple contact events with Hertzian and non-Hertzian events. Reconstruction cases a) Case 0. b) Case 1 (2x2).

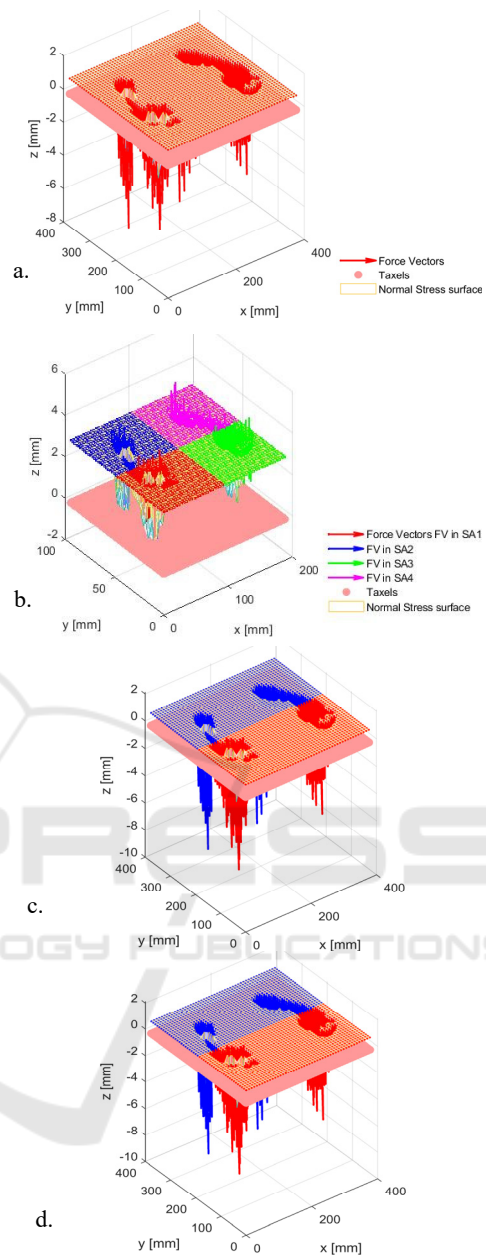


Figure 6: Results of partitioned force reconstruction contact events for a PPMs application. Reconstruction cases a) Case 0 (1x1). b) Case 1 (2x2). c) Case 2 (1x2). d) Case 3 (2x1).

4 DISCUSSION AND FUTURE WORKS

The model-driven on which this work is based was designed to reconstruct single contact events. Considering this limitation, it is not possible to guarantee the proper functioning of the proposed

partition approach for single contact events. This is because when dividing the sensor, it is not feasible to ensure that each subarray meets the centroid conditions since a single contact produces only one tension centroid and one compression centroid for the entire sensor.

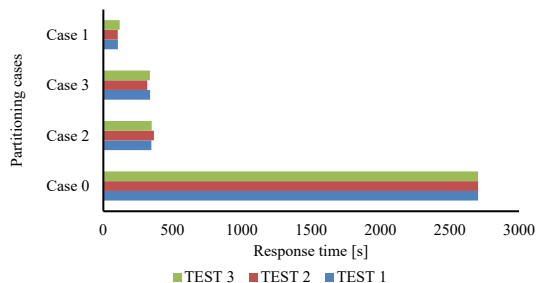


Figure 7: Response time for partitioning approach with a 48×48 taxels sensor.

Even for single contact events, the non-Hertzian contact analyzed had better behavior than the Hertzian one, since the first one allowed the partitioning of the sensor into two subarrays. This implies that non-Hertzian contacts have a greater expectation of being processed adequately with the proposed approach.

Applying the proposed approach shows a great decrease in the time required to rebuild the contact forces when the number of subarrays increases. This is because the order of operations in the matrix decreases for smaller subarrays, which improves the temporal response. For instance, for a 48×48 taxel matrix, without partitions (Case 0), the algorithm requires $(3 * 48 * 48) \times (6912)$ matrix operations. For Case 1 with four subarrays, the algorithm requires $(3 * 24 * 24) \times (1728)$ operations, while in Case 2 and Case 3, the algorithm involves $(3 * 24 * 48 = 3456)$ operations. This means that, despite the relatively high estimation errors obtained for this partitioning approach, its application for large tactile sensor arrays becomes attractive, since it significantly reduces the number of operations required.

The latency of the FPGA-based hardware implementation of the no partitioned model proposed by Seminara et al. (2015) is 1.6×10^{-6} s for processing an 8×8 size sensor. For its part, the software implementation developed herein for the above-mentioned model has a response time of 16.43 s, using the normal stress input data generated by applying Equation 3 and an 8×8 size sensor. This allows us to infer that given the reduction in the number of operations required for the proposed partitioning approach, the response times of the

hardware implementation are expected to be even lower than those reported by Seminara et al.

In multiple contact events, sensor 3 produces a good reconstruction of forces because this configuration allows meeting the centroid conditions for each analyzed subarray. This allows obtaining the optimal parameters μ_1 and μ_2 , which enables to use of this approach to properly model these contacts.

Future works include evaluating the reconstruction of single contact events for force feedback using the proposed partitioning approach on a hardware implementation considering applications such as electronic skin, manipulation tasks, and human-robot interaction.

5 CONCLUSIONS

The application of the proposed partitioning approach for a 48×48 taxel tactile sensor matrix shows a very significant decrease in the execution time, which goes from 2705.33 s to 109.63 s only, when performing the forces estimation using four subarrays of 24×24 taxels. The proposed partitioning approach to the contact force reconstruction in arrays of tactile sensors facilitates the decoding of the properties of the touched objects by considerably reducing the response time required to process the information provided by large tactile sensor arrays.

The validation of the partitioning approach depends on a prior verification of compliance with the centers of traction and compression for each analyzed subarray. Therefore, the proposed partition approach generates high errors for single contacts, while it presents tolerable errors for multiple contact events distributed in the subarrays.

Due to its characteristics of low computing power required and high execution speed, the proposed approach can be used in applications of human-robot interaction and force control loops in robotic manipulation, in which it is tolerable to work with an approximated knowledge of the properties of the touched object.

ACKNOWLEDGEMENTS

Authors thank the valuable support and collaboration of researchers of the COSMIC group at University of Genoa, Genova-Italy, and the VIE-UPTC for providing the funds to the international mobility to the University of Genoa.

REFERENCES

- Albert, A. (1972). *Regression and the Moore-Penrose Pseudoinverse*.
- Castro, F., Savaris, W., Araujo, R., Costa, A., Sanches, M., & Carvalho, A. de. (2020). Plantar Pressure Measurement System With Improved Isolated Drive Feedback Circuit and ANN: Development and Characterization. *IEEE Sensors Journal*, 20(19), 11034–11043. <https://doi.org/10.1109/JSEN.2020.2998700>
- Cimino, D. (2016). *Implementazione Hardware dedicata di Metodi di Data Processing per la Ricostruzione della Distribuzione di Forze di Contatto in Applicazioni Tattili*.
- Ciotti, S., Sun, T., Battaglia, E., Bicchi, A., Liu, H., & Bianchi, M. (2019). Soft tactile sensing: retrieving force, torque and contact point information from deformable surfaces. *2019 International Conference on Robotics and Automation (ICRA)*, 4290–4296. <https://doi.org/10.1109/ICRA.2019.8794087>
- Cirillo, A., Ficuciello, F., Natale, C., Pirozzi, S., & Villani, L. (2016). A Conformable Force/Tactile Skin for Physical Human–Robot Interaction. *IEEE Robotics and Automation Letters*, 1(1), 41–48. <https://doi.org/10.1109/LRA.2015.2505061>
- Dahiya, R. S., Metta, G., Valle, M., & Sandini, G. (2010). Tactile Sensing—From Humans to Humanoids. *IEEE Transactions on Robotics*, 26(1), 1–20. <https://doi.org/10.1109/TRO.2009.2033627>
- Dahiya, R. S., Mittendorf, P., Valle, M., Cheng, G., & Lumelsky, V. J. (2013). Directions Toward Effective Utilization of Tactile Skin: A Review. *IEEE Sensors Journal*, 13(11), 4121–4138. <https://doi.org/10.1109/JSEN.2013.2279056>
- Duong, L. Van, & Ho, V. A. (2021). Large-Scale Vision-Based Tactile Sensing for Robot Links: Design, Modeling, and Evaluation. *IEEE Transactions on Robotics*, 37(2), 390–403. <https://doi.org/10.1109/TRO.2020.3031251>
- Ibrahim, A., Pinna, L., & Valle, M. (2017). Interface Circuits Based on FPGA for Tactile Sensor Systems. *2017 New Generation of CAS (NGCAS)*, 37–40. <https://doi.org/10.1109/NGCAS.2017.60>
- Ito, D., Funabara, Y., Doki, S., & Doki, K. (2019). Control System Based on Contact Force Distribution for Wearable Robot with Tactile Sensor. *2019 IEEE/SICE International Symposium on System Integration, SII 2019*, 259–263. <https://doi.org/10.1109/SII.2019.8700383>
- Johnson, K. L. (1985). *Contact Mechanics*. <https://doi.org/DOI:10.1017/CBO9781139171731>
- Lambeta, M., Chou, P.-W., Tian, S., Yang, B., Maloon, B., Most, V. R., Calandra, R. (2020). DIGIT: A Novel Design for a Low-Cost Compact High-Resolution Tactile Sensor with Application to In-Hand Manipulation. *IEEE Robotics and Automation Letters*, 5(3), 3838–3845. <https://doi.org/10.1109/LRA.2020.2977257>
- Li, X., Li, W., Zheng, Y., Althoefer, K., & Qi, P. (2020). Criminisi algorithm applied to a gelsight fingertip sensor for multi-modality perception. *2020 IEEE/ASME International Conference on Advanced Intelligent Mechatronics, AIM 2020, 2020-July*, 190–195. <https://doi.org/10.1109/AIM43001.2020.9158799>
- Li, Y., Wang, B., Li, Y., Zhang, B., Weng, L., Huang, W., & Liu, H. (2019). Design and Output Characteristics of Magnetostrictive Tactile Sensor for Detecting Force and Stiffness of Manipulated Objects. *IEEE Transactions on Industrial Informatics*, 15(2), 1219–1225. <https://doi.org/10.1109/TII.2018.2862912>
- Masoumian, A., Montazer, M. C., Valls, D. P., Kazemi, P., & Rashwan, H. A. (2020). Using the Feedback of Dynamic Active-Pixel Vision Sensor (Davis) to Prevent Slip in Real Time. *6th International Conference on Mechatronics and Robotics Engineering, ICMRE 2020*, 63–67. <https://doi.org/10.1109/ICMRE49073.2020.9065017>
- Mohammadi, A., Xu, Y., Tan, Y., Choong, P., & Oetomo, D. (2019). Magnetic-based soft tactile sensors with deformable continuous force transfer medium for resolving contact locations in robotic grasping and manipulation. *Sensors (Switzerland)*, 19(22). <https://doi.org/10.3390/s19224925>
- Seminara, L., Capurro, M., & Valle, M. (2015). Tactile data processing method for the reconstruction of contact force distributions. *MECHATRONICS*, 27, 28–37. <https://doi.org/10.1016/j.mechatronics.2015.02.001>
- Trueeb, C., Sferrazza, C., & D’Andrea, R. (2020). Towards vision-based robotic skins: A data-driven, multi-camera tactile sensor. *3rd IEEE International Conference on Soft Robotics, RoboSoft 2020*, 333–338. <https://doi.org/10.1109/RoboSoft48309.2020.9116060>
- Wasko, W., Albin, A., Maiolino, P., Mastrogiovanni, F., & Cannata, G. (2019). Contact Modelling and Tactile Data Processing for Robot Skins. *SENSORS*, 19(4). <https://doi.org/10.3390/s19040814>
- XELA Robotics Inc. (n.d.). XELA Robotics | Sensing for the future. Retrieved April 19, 2020, from <https://www.xelarobotics.com/index?lang=en>
- Yuan, W., Zhu, C., Owens, A., Srinivasan, M. A., & Adelson, E. H. (2017). Shape-independent hardness estimation using deep learning and a Gelsight tactile sensor. *2017 IEEE International Conference on Robotics and Automation, ICRA 2017*, 951–958. <https://doi.org/10.1109/ICRA.2017.7989116>
- Zou, L., Ge, C., Wang, Z. J., Cretu, E., & Li, X. (2017). Novel Tactile Sensor Technology and Smart Tactile Sensing Systems: A Review. *SENSORS*, 17(11). <https://doi.org/10.3390/s17112653>